Clays and Clay Minerals, Vol. 39, No. 3, pp. 270–280, 1991.

"DEALUMINATION" AND ALUMINUM INTERCALATION OF VERMICULITE

JEAN-BAPTISTE D'ESPINOSE DE LA CAILLERIE AND JOSÉ J. FRIPIAT

Department of Chemistry and Laboratory for Surface Studies, University of Wisconsin–Milwaukee
P.O. Box 413, Milwaukee, Wisconsin 53201

Abstract—Dealumination of vermiculite was carried out using $(NH_4)_2SiF_6$ solutions. The dealuminated products were studied by high-resolution solid state ^{29}Si and ^{27}Al nuclear magnetic resonance. A decrease in the cation-exchange capacity (CEC) resulted from the partial removal of Al from the tetrahedral layer, which decreased the framework negative charge, and from the partial replacement of Mg by Al in the octahedral layer, which increased its positive charge contribution. The lowest CEC was obtained by swelling the structure with butyl-ammonium prior to the reaction with $(NH_4)_2SiF_6$. Thus, CECs in the range observed for beidellite were measured; however, the lowest $(Al/Si)^{IV}$ ratio was still more than twice as high as in beidellite. In addition, the dealumination reaction yielded noncrystalline silica as a by-product.

In contact with a solution of Al hydroxypolymer (Al_{13}), the dealuminated vermiculite showed no 18-Å reflection characteristic of Al_{13}-intercalated smectite; instead it showed an ill-defined interstratification. For some samples, however, a significant increase in the specific surface area (as much as 230 m^2/g) was observed, suggesting that an intercalation of Al moieties did occur. The ^{27}Al resonance spectra of the intercalated structure showed at least two components in octahedral coordination. On thermal activation, a resonance line attributable to pentacoordinated Al was observed.

Key Words—Aluminum, Cation-exchange capacity, Dealumination, Intercalation, Nuclear magnetic resonance, Vermiculite.

INTRODUCTION

Vermiculites are swelling trioctahedral micas containing Al-for-Si substitutions in tetrahedral layers and Al-, Fe-, and Ti-for-Mg substitutions in octahedral layers. They have been extensively studied, and an excellent review of their hydrated and cation-exchanged structures was recently published by de la Calle and Suquet (1988). Because of the tetrahedral and octahedral substitutions, the overall negative charge of the structure results from an imbalance between the negative charge of the tetrahedral layer and the excess positive charge of the octahedral layer.

The present work was undertaken to investigate (1) the possibility of lowering the net negative charge by substituting Al by Si in the tetrahedral layer, and (2) the possibility of pillaring the negative-charge-depleted vermiculite with the Al hydroxypolymer Keggin-like cation $Al_{13}O_4(OH)_{24}(H_2O)_{12}^{7+}$ (abbreviated here as Al_{13}). The procedure for substituting Si for Al in the tetrahedral layer has been used successfully on zeolites (Breck *et al.*, 1985). It consists of a mild treatment with $(NH_4)_2SiF_6$ in aqueous solution. The use of this reagent for modifying layered silicates was suggested earlier by Miyake *et al.* (1987).

As is shown below, the procedure suggested by Breck *et al.* (1985) resulted in a decrease of the cation-exchange capacity of vermiculite, the tetrahedral and octahedral compositions both being affected. Although Al species were introduced in the interlayer, as evidenced by a noticeable increase in specific surface area, pillaring in the classical was not achieved, inasmuch as no rationale d(00*l*) reflections with d(00*l*) $\approx$ 18 Å were observed. Instead, an ill-defined interstratified structure was obtained. This result is rich in information concerning the cation-exchange mechanism involving Al_{13}.

MATERIALS

Vermiculite

Two different samples of vermiculite were studied. Low-charge vermiculite from Benahavis having a half-unit cell composition (López Gonzalez and Barrales Rienda, 1972) of $Mg_{0.24}\ Ca_{0.03}\ (Si_{2.81}\ Al_{1.10}\ Fe^{3+}_{0.09})^{IV}\ (Mg_{2.46}\ Ti_{0.11}\ Fe^{3+}_{0.43})^{VI}\ O_{10}(OH)_2$ was ground to <2 μm (Stoke's radius). This material was converted into the sodium form by repeated contact with a 1 M NaCl solution and stirring at room temperature. The excess NaCl was washed out with distilled water, and the slurry was separated by centrifugation until Cl^- free.

High charge Llano vermiculite having a half-unit cell composition (Raussel-Colom *et al.*, 1980) of $Mg_{0.45}\ (Si_{2.78}\ Al_{1.22})^{IV}\ (Mg_{2.94}\ Al_{0.1}\ Ti_{0.02}\ Fe^{3+}_{0.01})^{VI}O_{10}(OH)_2$ was treated with dilute H_2SO_4 until no magnesite could be found in the X-ray powder diffraction diagram. It was then ground to <250- and <2-μm particle sizes. The more severe comminution did not noticeably affect the crystallinity, as evidenced by the similarity of the XRD patterns.

Both fractions were converted into the sodium form, as explained above. The Llano vermiculite was poorer

in paramagnetic centers than the Benahavis vermiculite. Consequently, the study of the Si-for-Al substitution by high-resolution, solid-state magic-angle spinning nuclear magnetic resonance (MAS-NMR) was possible, whereas such a study could not be achieved with the Benahavis vermiculite.

EXPERIMENTAL

Dealumination procedures

Several procedures, all based on the use of $(NH_4)_2SiF_6$, were applied and are designated by lower case a, b, and c. A following subscript will refer to experimental conditions, such as reaction time, reagents concentrations, and pH. Note that the solubilities of hexafluorosalts in water at 25°C are generally small. Linke (1965) quoted the following values: $(NH_4)_3AlF_6$, 0.04mole/liter; Na_3AlF_6, 0.002 mole/liter; Na_2SiF_6, 0.04 mole/liter; in contrast with $(NH_4)_2SiF_6$, 1.274 mole/liter and $MgSiF_6$, $\approx$ 1 mole/liter. Because these salts could have formed during the reaction, their solubility is an important and apparently overlooked factor.

Procedure "a" was suggested by Breck *et al.* (1985) for zeolites. About 0.5 g of Na vermiculite was suspended in 100 ml of a 1 M ammonium acetate buffer solution (pH = 7.8). An aqueous solution of $(NH_4)_2SiF_6$ was added dropwise (about 10 drops/minute) to the vigorously stirred suspension at ~60°C. The final concentration of the $(NH_4)_2SiF_6$ solution was adjusted such that the atomic ratio (Si added/Al^{IV} in vermiculite) was between 0.5 and 1. After the addition of $(NH_4)_2SiF_6$, the reaction was allowed to proceed for an additional 12 and 36 hr. After cooling, the solid was washed 10 times with distilled water and back exchanged into the sodium form, as described for the preparation of the initial Na-vermiculite.

In procedure "b" about 0.2 g of thoroughly ammonium exchanged vermiculite was suspended in 100 ml of a 0.007 M $(NH_4)_2SiF_6$, ammonium acetate buffer solution. The same conditions as in procedure "a" were maintained, except for the washing step, which was made with warm (~70°C) water. After the reaction, the solid was back exchanged with sodium. The rational for the difference between procedure "a" and procedure "b" was to avoid the presence of sodium in the reacting mixture and therefore to prevent the formation of the poorly soluble salts mentioned above.

In procedure "c" the Na-vermiculite was thoroughly exchanged with butyl-ammonium chloride (BACl) or fluoride (BAF) at a pH of 7.9. The sample was then stirred in a 0.01 M$(NH_4)_2SiF_6$ aqueous solution containing the corresponding butyl-ammonium chloride and fluoride salt (BACl or BAF) in an amount in excess of 5 or 50 times the cation-exchange capacity (CEC) of the solid. The other conditions were the same as in procedures "a" and "b." The reaction was carried out for 12 hr at ~60°C under vigorous stirring. The product was washed thoroughly with water at 25°C. In one experiment, the product was washed with a NaOH solution at pH = 9. The rational for procedure "c" comes from the observation that the ammonium-exchanged Llano vermiculite did not swell extensively in water, whereas it swelled in BACl and BAF solutions. Thus, procedure "c" combined the advantages of eliminating the sodium and of making the interlayer space more available to $(NH_4)_2SiF_6$.

Pillaring procedure

Attempts were made to pillar some of the dealuminated vermiculite samples with Al_{13} following the optimized procedure described by Schutz *et al.* (1987) or Plee *et al.* (1987).

Characterization techniques

Cation-exchange capacity. CECs were obtained by displacing the exchangeable Na^+ with ammonium acetate as described by Bain and Smith (1987). The Na content so extracted in the exchange solution was analyzed by atomic emission spectroscopy at 589 nm, as described by Thompson and Reynolds (1978).

Aluminum content. Samples were dissolved in a platinum crucible according to the HF-H_2SO_4 method (Angino and Billings, 1972). The Al content was determined by back-titration of Al-EDTA complex (Farrah and Moss, 1966).

X-ray powder diffraction (XRD). A home-computerized Philips goniometer and Ni-filtered CuK_α radiation were used to record the XRD pattern of oriented films of untreated and treated vermiculites. The exit slit was 1°; the entrance slit was 0.006 inches.

Magic-angle spinning nuclear magnetic resonance (MAS-NMR). The ^{27}Al and ^{29}Si NMR one-pulse signals were recorded at 130.3 and 99.3 MHz, respectively. For ^{29}Si, pulse width of about 5 μs, acquisition time of 25 ms, and 2-s delay time were the standard conditions. For ^{27}Al, the pulse width was between 1 and 2 μs, the acquisition time was 51 ms, and the delay time was <0.1 ms. For both nuclei, the number of accumulations was between 5000 and 10,000. The chemical shifts of the ^{29}Si and ^{27}Al resonance lines were referred to tetramethylsilane (TMS) and a 0.1 M $AlCl_3$ solution, respectively.

Surface area measurements. The specific surface area was measured in a volumetric all-glass BET instrument using N_2 as the adsorbate at −196°C. The samples were pretreated at 100°C under vacuum prior to N_2 adsorption. Some were thermally activated as described below.

RESULTS AND DISCUSSION

Dealumination

The measured CEC of the coarse fraction (>250 μm) of the Llano and of the fine fraction (<2 μm) of the Benahavis samples, not corrected for hydration, were 215 and 110 meq/100 g, respectively. Dealumination procedure "a" was applied to the Llano sample for 12, 24, and 36 hr. The variation of the relative CEC (i.e., CEC at time t/initial CEC) is shown in Figure 1. The formal ratio R = (Si added/Al^{IV}), is 1 in these experiments. A correlation is apparent between the decrease of the relative CEC and the square root of the reaction time (hr). The absolute error in the relative CEC is 0.06, and the slope is $-0.11\ hr^{-1/2}$. This $\sqrt{t}$ relationship suggests that the reaction was diffusion limited; however, the diffusion of the reagent within the interlayer was apparently not limiting. Otherwise, a much smaller decrease of the CEC for the coarse (<250 μm) Llano sample used in procedure "a" (samples $Llano_a$ in Figure 1), as compared to the fine (<2 μm) fraction used in procedure "b" (sample $Llano_b24$), should have been observed. Hence, the results in Figure 1 suggest that the rate-limiting step was the diffusion of Al^{IV} out of, or the diffusion of Si^{IV} into the tetrahedral layer. In addition, dealumination by either procedure "a" or "b" did not seem to have brought about significant differences.

https://doi.org/10.1346/CCMN.1991.0390307 Published online by Cambridge University Press

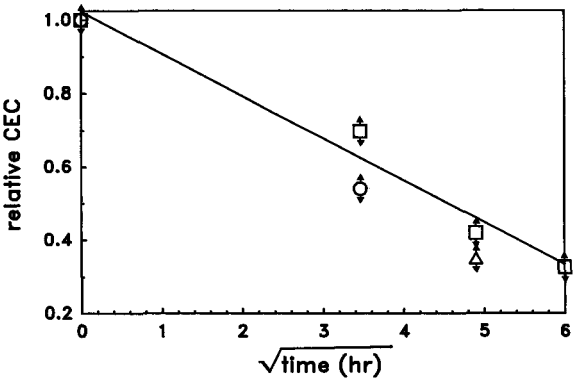

Figure 1. Decrease of observed relative cation-exchange capacity (CEC) vs. square root of reaction time. R = [Si added as $(NH_4)_2SiF_6/(Al)^{IV}$] = 1; temperature = 60°C. From left to right: (□) Llano, $Llano_a12$, $Llano_a24$, $Llano_a36$; (○) Benahavis, $Benahavis_a$; (△) $Llano_b24$. Solid line = linear regression obtained for $Llano_a$ α $\sqrt{t(hr)}$; arrows represent errors in measured relative CEC.

To this point, the dealumination process behaved as expected. Consequently the material obtained after 36 hr of treatment "a" of the coarse Llano sample ($Llano_a36$) was carefully inspected by ^{29}Si and ^{27}Al MAS-NMR. The relative CEC of this sample was 0.33. The deconvolution of the ^{29}Si and ^{27}Al signals are displayed in Table 1. What is not shown in this table is the noticeable contribution of a broad ^{29}Si line centered at −111 ppm, corresponding to a ^4Q environment. The initial sample had a narrow and weak contribution at about this frequency, which can be attributed to residual quartz or cristobalite.

The ratio $(Al/Si)^{IV}$ in the vermiculite structure was obtained quite accurately from the equation

$$\left(\frac{Al}{Si}\right)^{IV} = \sum_{n=0}^{n=3} \frac{n}{3} I(Si, nAl), \qquad (1)$$

where I(Si,nAl) is the relative intensity of the $^3Q(Si,nAl)$ contribution to the overall intensity of the framework ^{29}Si. The results in Table 1 were duplicated for other samples (*vide infra*).

Table 1. Magic-angle spinning nuclear magnetic resonance results obtained by deconvolution of the ^{29}Si and ^{27}Al spectra.

Vermiculite sample[1]	Integrated intensities				
	^3Q (Si,2Al)	^3Q (Si,1Al)	^3Q (Si,0Al)	$(Al/Si)^{IV}$[3]	(Al^{VI}/Al_{total})
Na-Llano	41	53	6	45%	10%
Na-$Llano_a$ 36[2]	28	49	22	35%	16.5%
δ(TMS) (ppm)	−84	−88	−93		
$\delta(Al^{3+})$ (ppm)				68	3

[1] See text for descriptions.

[2] This is the coarse Llano submitted to dealumination procedure "a" during 36 hr (cation-exchange capacity = 70 meq/100 g).

[3] Obtained using the Lowenstein rule (Eq. 1).

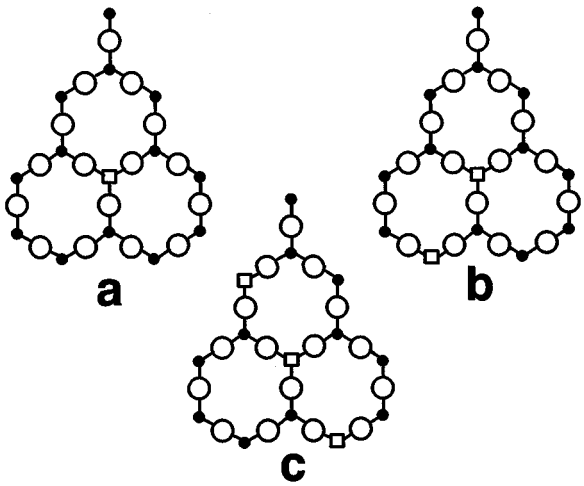

Figure 2. Schematic representation of effect of Al^{IV}-by-Si^{IV} substitution mimicking trend (described in Table 1) in variation of silicon environment. □, Al; ●, Si; ○, O. (a) Al^{IV} has no Al^{IV} as second neighbor. Its substitution by Si^{IV} leads to the creation of four [Si,3Si] sites and the disappearance of three [Si,1Si,2Al] sites. (b) Al^{IV} has one Al^{IV} as second neighbor. Its substitution by Si^{IV} leads to the creation of three [Si,3Si] sites and the disappearance of one [Si,1Si,2Al] and of one [Si,2Si,1Al] sites. (c) the Al^{IV} has two Al^{IV} as second neighbor. Its substitution by Si^{IV} leads to the creation of one [Si,2Al,1Si] and of two [Si,3Si] sites and the disappearance of two [Si,2Si,1Al] sites.

From the data reported to this point, dealumination seems to have affected significantly the site [Si,1Si,2Al], i.e., a silicon site surrounded by one Si and two Al atoms, as well as the site [Si,3Si]. The relative intensity of the latter increased at the expense of the former. This observation is schematically accounted for in Figure 2, in which the [Si,3Al] site has been neglected because its contribution was too weak to be clearly detected.

If a maximum of two Al per pseudo-hexagonal ring existed for reasons of electrostatic stability described by Herrero (1985), the substitution of one of them by Si increased the [Si,2Si,1Al] contribution, whereas the substitution of Al by Si in this environment increased the [Si,3Si] contribution. Hence, if substitution occurred at random, the relative intensity of the (Si,1Al) environment did not change much, as observed in Table 1.

The overall $(Al/Si)^{IV}$ ratio decreased from 45% to 35%. If the dealumination reaction affected only the tetrahedral layer, the relative CEC should have decreased from 1 to 0.84 instead of from 1 to 0.33, as was observed. On the other hand, the ratio of the six-fold coordinated Al signal to the overall ^{27}Al signal increased *significantly* from 10% to 16.5% (Table 1). This information is only qualitative because the two ^{27}Al resonances at about −68 and about 3 ppm do not behave similarly under the radio-frequency excitation. According to the chemical formula, in the initial ver-

https://doi.org/10.1346/CCMN.1991.0390307 Published online by Cambridge University Press

miculite this ratio was about 9%. Thus, some of the Al extracted from the tetrahedral layer was probably not washed out as $(NH_4)_3AlF_6$. The solubility of this salt was low, as indicated above, but the dilution of the reacting solution and the subsequent washings should have removed it. In addition to observing an increase in the (Al^{VI}/total Al) ratio, the very significant increase of a ^4Q component in the ^{29}Si spectrum, which indicates the formation of extra-framework silica, cannot be neglected. If some kind of silica gel was formed at the expense of the reagent, it could have combined with the extracted Al, resulting in the formation of a noncrystalline silica-alumina whose ^{29}Si resonance would have been split into a $^4Q(Si,4Si)$ signal at about -110 ppm and a weaker $^4Q(Si,3Si,1Al)$ signal between -100 and -105 ppm (Man *et al.*, 1990). If this gel had a low CEC, the overall observed CEC would have been less than what could have been predicted from the $(Al/Si)^{IV}$ ratio in the vermiculite framework.

From these conditions, the lowering of the CEC may have resulted from three factors; (1) the removal of Al^{IV} from the tetrahedral layer, (2) the translocation of extracted Al from the tetrahedral layer into the octahedral layer ($Al^{IV} \rightarrow Al^{VI}$) and extraction of Mg from the octahedral layer, and, (3) formation of extra-framework silica. The $Al^{IV} \rightarrow Al^{VI}$ translocation would have increased the positive charge in the octahedral layer and lowered the overall negative charge of the structure, already depleted by the Al^{IV}-by-Si^{IV} substitution in the tetrahedral layer. The following scheme accounts for different reactions that could have occurred. The octahedral substitutions by other elements than Al have been neglected for sake of clarity.

(1) cation substitution in the tetrahedral layer:

$$M^+_{(x-y)}[Si_{(4-x)}, Al_x]^{IV}[Mg_{(3-y)}, Al_y]^{VI}O_{10}(OH)_2 + (x - x')(NH_4)_2SiF_6 \rightarrow (NH_4^+)_{(x'-y)}[Si_{(4-x')}, Al_{x'}]^{IV}[Mg_{(3-y)}, Al_y]^{VI}O_{10}(OH)_2 + [M_{(x-y)}(NH_4)_{(2x-3x'+y)}][AlF_6]_{(x-x')}. \quad (2)$$

If M^+ is NH_4^+ (procedure "b"), the last right-hand member is $(x - x')(NH_4)_3AlF_6$.

(2) cation substitution in the octahedral layers, the last right-hand member in (2) being abbreviated $(x - x')M_3AlF_6$.

$$(x - x')M_3AlF_6 + (NH_4^+)_{(x'-y)}[Si_{(4-x')}, Al_{x'}]^{IV} \cdot [Mg_{(3-y)}, Al_y]^{VI}O_{10}(OH)_2 \rightarrow (NH_4^+)_{(x'-y')}[Si_{(4-x')}, Al_{x'}]^{IV}[Mg_{(3-y')}, Al_{y'}]^{VI}O_{10}(OH)_2 + [(x - x') - (y - y')]NH_4MgAlF_6 + [(x - x') - (y - y')]M_3AlF_6, \quad (3)$$

where $y - y' \leq x - x'$.

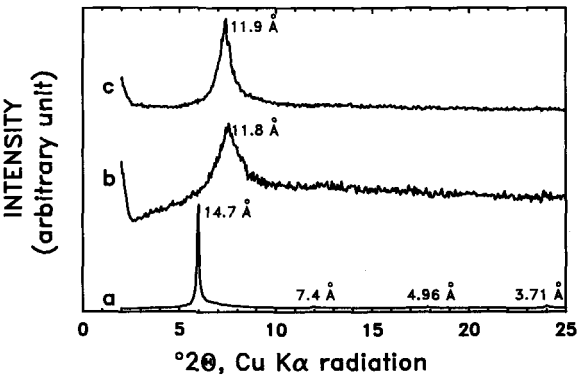

Figure 3. X-ray powder diffraction (CuK_α) patterns of oriented samples: a, Na-Benahavis; b, Na-Benahavis$_a$24, R = [Si added as $(NH_4)_2SiF_6/(Al)^{IV}$] = 0.5, relative CEC = 0.64; c, Na-Benahavis$_a$12, R = 1, relative CEC = 0.54. Samples were equilibrated with atmospheric moisture at room temperature.

Finally, the hydrolysis of $(NH_4)_2SiF_6$ can be written as

$$(NH_4)_2SiF_6 + 2\ H_2O \rightarrow 4\ HF + 2\ NH_4F + SiO_2. \quad (4)$$

Note that NH_4MgAlF_6 is insoluble and easily characterized in an XRD pattern by sharp reflections at 5.77, 3.01, 2.88, 2.03, 1.92, and 1.76 Å. For example, the reaction of $(NH_4)_3AlF_6$ with the magnesium mineral sepiolite leads to extensive formation of NH_4MgAlF_6, easily identified by XRD.

By and large, the dealumination of vermiculite is not a simple, neat reaction. The formation of silica having a $^4Q(Si,4Si)$ resonance at -111 ppm yields HF (Eq. (4)). This acid may extract Mg from the octahedral layer. Al may also be extracted from the tetrahedral layer sites by HF and may fill the octahedral site left vacant by Mg. A fraction of the extracted Al can also be washed out as M_3AlF_6 or precipitated as NH_4MgAlF_6 (Eq. (2)), if the solubility product is reached.

The XRD lines of NH_4MgAlF_6 were not observed in the XRD diagram represented in Figure 3 and obtained for the Na-Benahavis and Na-Benahavis$_a$ samples at two different degrees of dealumination. The three samples were equilibrated at room temperature with atmospheric moisture. Whereas the initial Na-Benahavis sample showed the reflection of the two-layer hydrate, the dealuminated samples swelled to about 11.8 Å. This spacing is typical of the one-layer hydrate. The reduced swelling was expected from the decrease of the layer charge. An appreciable loss of crystallinity was evident from the broadening of the 001 reflection. Note, that if NH_4MgAlF_6 had been washed out, M_3AlF_6 with M = Na or NH_4, which is more soluble, would have been removed as well upon washing.

Thus, from the above data, an appreciable fraction of the tetrahedral aluminum was probably transferred

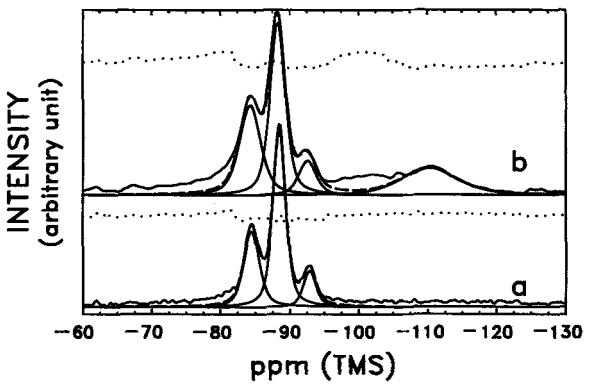

Figure 4. Example of deconvolution of the ^{29}Si magic-angle spinning nuclear magnetic resonance (MAS-NMR) spectra into 50% gaussian, 50% lorentzian lines. The two samples shown here have about the same $(Al/Si)^{IV}$ framework composition. (a) Mg-Llano vermiculite; (b) sample $Llano_cBAC150(b)$ (Table 2). Full line: observed spectrum. Dashed line: sum of the ^nQ contributions. There are three contributions for Llano: $^3Q(Si,2Al)$, $^3Q(Si,1Al)$ and $^3Q(Si,0Al)$ from left to right. $Llano_cBAC150(b)$ shows the additional ^4Q contribution at about −110 ppm attributed to extra-framework silica. Dotted lines = residuals.

by combined steps (1) and (2) into the octahedral layer. Reactions (2) and (3) are only formal chemical representations. It may be that Al translocation occurs without redissolution. On the basis of this hypothesis, relative CEC can be calculated in the following way: per half unit cell (½ uc), the CEC is proportional to $(x - y)$, and the relative CEC is proportional to $(x - y)/(x_0 - y_0)$, where x_0 and y_0 refer to the initial composition of the vermiculite structure. In addition, because extra-framework SiO_2 is formed during the dealumination process, the relative CEC is

$$\text{relative CEC} = \frac{(x - y)}{(x_0 - y_0)} \cdot \frac{^3Q}{Si(t)}, \qquad (5)$$

where ^3Q is the sum of the intensities of the three ^{29}Si framework contributions and Si(t) is the overall intensity of the ^{29}Si MAS-NMR signal. Figure 4 illustrates a reaction in which the precipitation of extra-framework silica (reaction 4) was evidenced by a noticeable contribution at about −111 ppm in the ^{29}Si MAS-NMR spectrum. This precipitation occurs in spite of the fact that in this particular sample ($Llano_cBAC150(b)$ in Table 2) $r(Si) = (Al/Si)^{IV}$ did not significantly decrease. In Eq. (5), x and y can be obtained as follows. Let us define

$$r(Si) = \frac{Al^{IV}}{Si^{IV}} \qquad (6)$$

and

$$r(Al) = \frac{Al^{VI}}{Al^{IV}}, \qquad (7)$$

where r(Si) is given by Eq. (1). r(Si) can be obtained quite accurately from the ^{29}Si MAS-NMR spectrum. Because, per ½ uc, $Al^{IV} + Si^{IV} = 4$,

$$x = \frac{4r(Si)}{1 + r(Si)}, \qquad (8)$$

and

$$y = x \cdot r(Al), \qquad (9)$$

assuming that all Al^{VI} is within the vermiculite framework. r(Al) can be estimated from the deconvolution of the ^{27}Al MAS-NMR spectrum, but this procedure is not very accurate. Indeed, ^{27}Al being a quadrupolar nucleus, and the quadrupolar coupling constant of Al^{IV} and Al^{VI} being different, the widths of the radio frequency pulses produced to observe the maximum intensity of the ±½ resonance line are different. Another way to estimate y in the dealuminated sample is:

$$y = y_0 + (x_0 - x). \qquad (10)$$

In Eq. (10), no Al is assumed to have leached out in the dealumination process. The advantage of using Eq. (10) vs. Eq. (9) is that the approximate value of r(Al)

Table 2. Observed and calculated relative cation-exchange capacity (CEC) in dealuminated Llano vermiculite.

Vermiculite sample[1]	Obs. rel. CEC	Cal. rel. $CEC_{(1)}$[5]	Calc. rel. $CEC_{(2)}$[6]	r(Si)	r(Al) obs.	$^3Q/Si(t)$	pH reaction	Framework rel CEC[7]
Na-Llano	1.00	1.00	1.00	0.45	0.12	1.00		1
$Llano_c$ BAF5	0.32	0.22	0.31	0.33	0.57	0.56	5.5	0.57
$Llano_c$ BAF50	0.33	0.3	0.24	0.30	0.40	0.58	6.4	0.57
$Llano_a$ 36[2]	0.33	0.53	0.44	0.35	0.20	~0.7	5.5	0.47
$Llano_c$ BAC15	0.46	0.35	0.55	0.45	0.44	0.55	4.3	0.88
$Llano_c$ BAC150	0.03	~0	0.18	0.32	≥1	0.36	4.2	0.08
$Llano_c$ BAC150 (b)[3]	n/a	0.58	0.60	0.41	0.15	0.77	5.5	n/a
$Llano_c$ BAC150 (c)[4]	0.98	0.90	0.86	0.39	0.13	1.00	7.3	~0.98

[1] See text for descriptions.
[2] This is the sample analyzed in Table 1.
[3] This sample has been washed several times with an NaOH aqueous solution at pH = 9 to remove colloidal silica.
[4] Same preparation as $Llano_c$ BAC150 sample, except for pH = 7.3.
[5] Using Eq. (9).
[6] Using Eq. (10).
[7] Framework relative CEC is obs. rel. CEC/[$^3Q/Si(t)$].

https://doi.org/10.1346/CCMN.1991.0390307 Published online by Cambridge University Press

Table 3. Chemical determination of Al contents (10^{-3} mole/g of material).

Vermiculite sample[1]	Si added/ Al^{IV} framework	Al content	Relative cation-exchange capacity	Relative Al content
Llano		3.47	1	1
$Llano_a12$	1	3.15	0.7	0.96
$Llano_a24$	1	3.1	0.42	0.945
$Llano_a36$	1	3.27	0.32	0.99
$Benahavis_a24$	0.5	2.75	0.63	1.03
$Benahavis_a12$	1	1.95	0.54	0.73

[1] See text for descriptions.

obtained from ^{27}Al NMR is not needed and that $y_0 = x_0 \cdot r_0(Al)$ is obtained quite accurately from the chemical analysis of the starting material.

Thus, the relative CEC can be calculated using Eq. (5) in which x is obtained from Eq. (8) and y is either obtained from Eq. (9) or from Eq. (10). In the last procedure:

$$\text{relative CEC} = \frac{2x - [1 + r_0(Al)]x_0}{[1 - r_0(Al)]x_0} \cdot \frac{^3Q}{Si(t)}, \quad (11)$$

whereas in the first (i.e., Eq. (9)):

$$\text{relative CEC} = \frac{[1 - r(Al)]x}{[1 - r_0(Al)]x_0} \cdot \frac{^3Q}{Si(t)}. \quad (12)$$

To check the validity of Eq. (5)–(12) and the underlying hypothesis that the actual reaction occurring between the vermiculite and $(NH_4)_2SiF_6$ was a two-step reaction, seven samples of dealuminated vermiculite, obtained according to procedures "c" (six samples) and "a" (one sample), were studied using ^{29}Si and ^{27}Al MAS-NMR, and by measuring the CEC. The results are summarized in Table 2. Note that procedure "c" was applied to the <2-μm fraction of the Llano vermiculite. The chemical determination of the Al contents shows that little, if any, Al was removed by the reaction with $(NH_4)_2SiF_6$. Per gram of starting material, the Al contents of the two samples were 3.28×10^{-3} and 2.68×10^{-3} mole, according to the structural formulae. As shown in Table 3, after reaction, the Al contents decreased by less than 5% in the $Llano_a$ series of reacted materials and in the $Benahavis_a24$ sample. The experimental error in the Al analyses was in the order of ±5%. The $Benahavis_a12$ sample was somewhat more depleted in Al, but no correlation between the relative CECs and the Al contents in the five analyzed samples was obvious. In addition, for the $Llano_a36$ sample, for which chemical composition of the reacted material could be calculated from the NMR data, good agreement exists between the calculated and the measured absolute Al contents. Indeed, from Table 2, the composition of this material should be:

$$0.7\ [(Si_{2.94}Al_{1.04})^{IV}(Mg_{2.8}Al_{0.2})^{VI}O_{10}(OH)_2] + 0.3\ SiO_2,$$

from which the calculated Al content is 3.15×10^{-3} mole/g. The measured Al content is 3.27×10^{-3} mole/g. If the Al extracted from the tetrahedral layer had been washed out, the Al content in the solid would have been 2.44×10^{-3} mole/g.

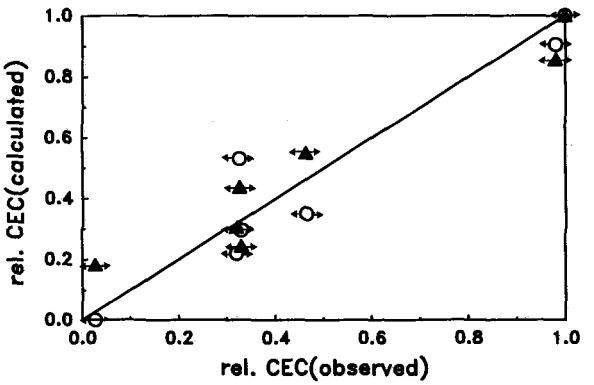

Figure 5. Correlation between observed relative cation-exchange capacity (CEC) and the calculated relative CEC shown in Table 2. Arrows show experimental error in measured relative CEC. Error in the calculated relative CEC is at least as large as in observed CEC. (○) calculated relative CEC using $r(Al)_{NMR}$ and Eq. (12); (▲) calculated relative CEC using Eq. (11).

The relationship between the relative CEC calculated in using either Eq. (9), relative $CEC_{(1)}$, or Eq. (10), relative $CEC_{(2)}$, and the observed relative CEC is shown in Figure 5. No systematic difference between the $CEC_{(1)}$ and $CEC_{(2)}$ sets of values was noted. Therefore, the $r(Al)_{obs}$ value obtained from ^{27}Al NMR is within the uncertainty of the other steps of the calculation. Some examples of deconvolution of ^{27}Al MAS spectra are shown below (see Figure 10 and Table 4). In addition, the calculated relative CECs are within ± 0.1 of the observed relative CECs. This large margin of error may be due to several reasons; possibly the residual hydration of the air-dried dealuminated minerals was not the same as that of the original mineral, as shown on Figure 3. Overestimating the hydration can lead to underestimating the CEC. Also, the correction introduced by multiplying $(x - y)/(x_0 - y_0)$ by $^3Q/Si(t)$ in Eq. (5) is a rough estimate because the ^4Q ^{29}Si NMR line was rather broad.

Figure 6 shows the XRD obtained for the $Na\text{-}Llano_b$ samples with increasing degrees of dealumination. Their observed relative CECs are shown in Figure 1. At equilibrium with atmospheric moisture, the starting Na-vermiculite samples had rational d(001) basal spacings at 14.6 ± 0.1 Å and the XRD reflections were sharp. As dealumination proceeded the widths of the 00*l* reflections increased. Samples having relative CECs <0.7 had d(001) values of 12 ± 0.2 Å under the same conditions of humidity. This decrease in d(001) of the Na samples is in agreement with the observation reported in Figure 3. Reducing the layer charge limited the swelling to the one-layer hydrate in both vermiculite samples. The broad reflection at about 3.49 Å intensified

https://doi.org/10.1346/CCMN.1991.0390307 Published online by Cambridge University Press

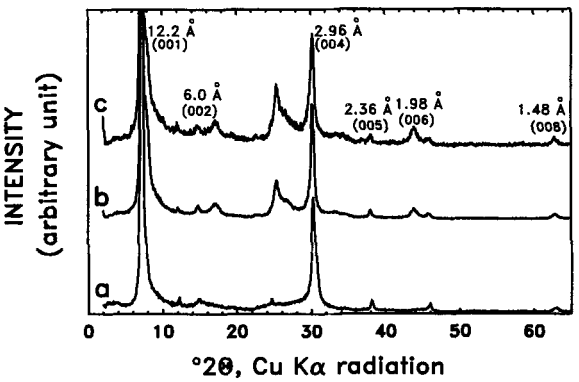

Figure 6. X-ray powder diffraction patterns of dealuminated $Llano_a$. From (a) to (c) are the diffraction patterns of samples Na-$Llano_a$12, Na-$Llano_a$24 and Na-$Llano_a$36 (see also Figure 1).

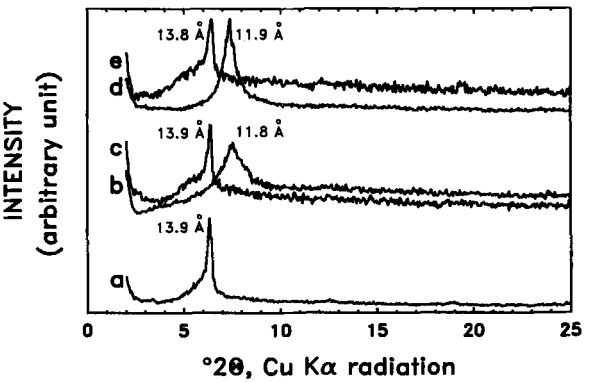

Figure 7. X-ray powder diffraction patterns of Na-Benahavis, Na-$Benahavis_a$24, and Na-$Benahavis_a$12 samples unreacted and reacted with Al_{13} solution, air dried and equilibrated at atmospheric moisture (see text). (a) Na-Benahavis sample reacted with Al_{13}; (b) Na-$Benahavis_a$24 sample; (c) Na-$Benahavis_a$24 sample reacted with Al_{13}; (d) Na-$Benahavis_a$12 sample; (e) Na-$Benahavis_a$12 sample reacted with Al_{13}. The specific area of Na-$Benahavis_a$12 sample reacted with the Al_{13} solution is 286 m^2/g after outgassing at 85°C, and 236 m^2/g after outgassing at 300°C.

as dealumination (obtained by procedure "b") increased. This peak was not identified.

Also, the 060 reflections of the dealuminated samples did not shift from their position in the XRD patterns of initial vermiculite (d(060) ≈ 1.54 Å). For most dioctahedral minerals, d(060) ≈ 1.49 Å. Thus, no intermediates between dioctahedral and trioctahedral structures nor a mixture of both were formed on dealumination.

Possibly, most of the reaction led to the formation of a noncrystalline phase. The ^{29}Si MAS-NMR spectra suggests that this transformation did not bring about a major contribution, as long as the pH of the reaction was not too low.

Lowering the pH had two consequences: (1) it decreased the $^3Q/Si(t)$ ratio, which means that reaction 5 was favored; (2) it favored the removal of the octahedral Mg and eventually the translocation of Al. Conclusions regarding the translocation of Al are supported by the data in Table 2, with the exception of the $Llano_cBAC150$ sample, in which for an unknown reason, the $r(Al)_{obs}$ was much higher than for all other samples and in which the observed CEC was almost zero. As long as the pH > 5.5, amorphization does not take place to any great extent.

From the above discussion, the hypothesis that there is no overall loss of aluminum but a transfer of Al from the tetrahedral to the octahedral layer appears to be correct, at least to the first approximation. Thus, "aluminum translocation" more adequately represents the actual reaction mechanism than does "dealumination."

With regard to the lowering of the structural charge, designated as framework relative CEC in Table 2, the residual framework CEC is always ≥0.5; i.e., the absolute CEC of the Llano dealuminated material is never less than about 125 meq/100 g. In addition, the lowest observed r(Si) is about 0.3, which means that the lowest x is about 0.92 Al^{IV} per ½ uc. The decrease of the negative tetrahedral charge is very limited, inasmuch as the starting material contains 1.22 Al^{IV}. Therefore, the so-called dealuminated material is still very rich in tetrahedral substitutions compared, for example, with beidellite, in which the Al^{IV} content, per ½ uc, is about 0.5 Al^{IV}. The residual framework CEC of the most dealuminated Llano sample is quite large, compared with ~ 90 meq/100 g for beidellite (Plee *et al.,* 1985). The dealuminated Benahavis vermiculite may have a smaller framework CEC, but because the paramagnetic centers in the structure preclude NMR investigations, the residual structural composition cannot be calculated.

Pillaring

Repeated attempts to pillar dealuminated vermiculite with Al_{13} failed in the sense that rational interlayer spacings in the range of 18 Å were never produced. On the other hand, experimental evidence was obtained to show that the $Benahavis_a$, $Llano_b$, and $Llano_c$ dealuminated samples reacted with Al_{13} solutions.

For examples, initial Na-vermiculite from Benahavis and dealuminated Na-$Benahavis_a$24 (Si added/Al^{IV} = 0.5) and Na-$Benahavis_a$12 (Si added/Al^{IV} = 1) having relative CECs of 1, 0.64, and 0.54, respectively, were reacted with Al_{13} solutions containing about 30 meq Al^{3+}/g clay. They were dialyzed as described in the experimental section. As shown in Figure 7, after reaction and drying at room temperature, all three samples were characterized by an XRD reflection at ~13.9 Å, whereas a reflection at 11.9 Å was observed for the dealuminated samples under the same condition, i.e., at equilibrium with atmospheric moisture. In addition, the XRD patterns of the dealuminated samples showed

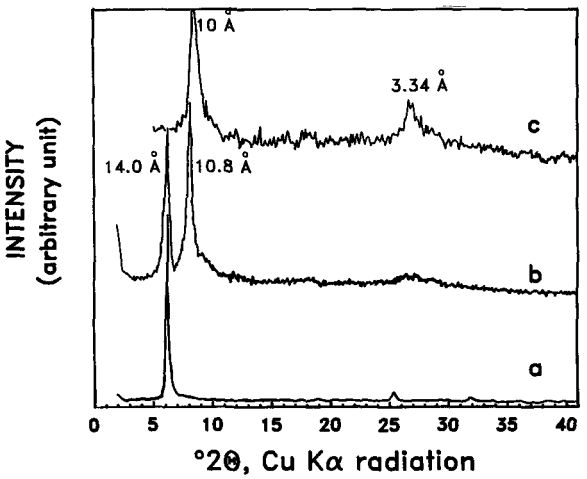

Figure 8. X-ray powder diffraction patterns of Na-Llano$_b$ sample reacted with Al_{13} solution. (a) dried at room temperature; (b) calcined for 1 hr at 350°C; (c) calcined for 1 hr at 500°C.

a shoulder on the low-angle side of the 13.9 Å peak. The XRD pattern of the dealuminated Llano$_b$12 (relative CEC = 0.42) reacted at room temperature with Al_{13} (Figure 8) showed one sharp peak at 14 Å. After 1 hr calcination at 350°C, two 001 peaks at ~14 and 10.8 Å were observed. Further calcination at 500°C for 1 hr yielded a broad reflection in the XRD pattern having a maximum at 10.5 Å and a weak reflection at 3.34 Å. The fine-grained (<2μm) dealuminated Llano$_c$ BAC150 sample contacted with Al_{13} gave a sharp peak at 14 Å on drying at room temperature, whereas the basal reflection broadened and shifted to lower spacing after the sample was heated at 350°C.

Obviously, an interlayer spacing of ~4.5 Å, i.e., the basal spacing (14 Å) minus the thickness of the vermiculite layer (9.5 Å), was too small to accommodate the bulky Al_{13} cation with its four planes of oxygen. Hence, the XRD spectra in Figures 7 to 9 suggest that another Al species was intercalated. A 14-Å spacing could have been associated with the two-layer hydrate of Al^{3+} cation obtained by the hydrolysis of Al_{13}. In other words, the equilibrium

$$Al_{13} \leftrightharpoons \cdots \leftrightharpoons \text{dimer} \leftrightharpoons Al^{3+} \qquad (13)$$

would have been shifted towards the right if the structure selectively adsorbed Al^{3+}. On thermal activation at >350°C, the interlayer cation loses its hydration layer and the basal spacing shrinks to about 10.5 Å. Thus, the presence of Al^{3+} alone in the interlayer cannot explain the low-angle shoulder.

Surface area measurements were carried out on the Benahavis$_a$12 sample (relative CEC = 0.54) that had been contacted with the Al_{13} solution and dialyzed. After outgassing at 85°C, the specific surface area was 286 m^2/g; it decreased to 236 m^2/g after outgassing at 300°C in vacuum. Because the surface area of the starting Benahavis sample was <1 m^2/g and that of the dealuminated sample was <20 m^2/g, interlayer aluminum moieties clearly were present after the treatment with Al_{13}. Plee (1984) reported similar results, but lower surface areas on contacting the Benahavis vermiculite with Al_{13}.

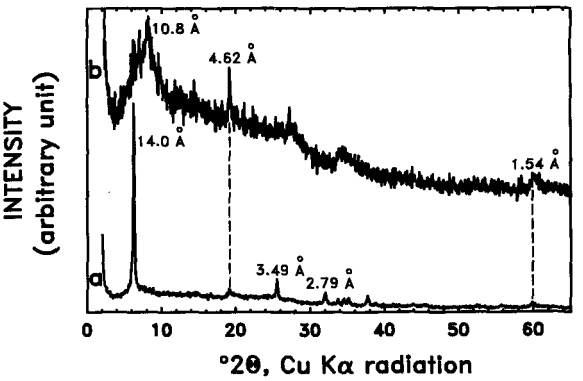

Figure 9. X-ray powder diffraction of dealuminated Llano$_b$BAC150(b) sample (see Table 2) reacted with Al_{13} solution. (a) dried at room temperature (b) calcined for 1 hr at 350°C.

To obtain information on the nature of these Al moieties, the ^{27}Al spectra of Llano$_c$BAC150(b) contacted with Al_{13} (XRD pattern shown in Figure 9) and dried at room temperature or calcined at 350°C were deconvoluted, as shown in Figure 10.

In the room-temperature dried sample, the r(Al)=(Al^{VI}/Al^{IV}) ratio increased from about 15% in the dealuminated sample (spectrum a) to 48% in the intercalated sample (spectrum b). Such an increase can

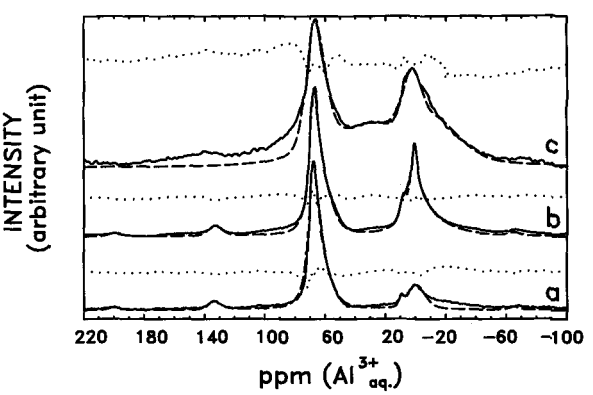

Figure 10. Deconvolution of ^{27}Al magic-angle spinning nuclear magnetic resonance spectra into 50% gaussian, 50% lorentzian lines. (a) Llano$_c$BAC150(b) sample; (b) intercalated Llano$_c$BAC150(b) sample dried at room temperature; (c) same after heating at 500°C. Solid lines = observed spectra. Dashed lines = sum of Al^{IV} contribution at ~68 ppm and two Al^{VI} contributions in spectrum (b), or three Al^{VI} contributions in spectrum (c) (see text). In spectrum (c), there is an additional contribution at ~30 ppm. The spinning side bands are easily observable on the left of the Al^{IV} contribution (at ~68 ppm). Dotted lines = residual.

https://doi.org/10.1346/CCMN.1991.0390307 Published online by Cambridge University Press

Table 4. Deconvolution of ^{27}Al magic-angle spinning nuclear magnetic resonance spectra.

Vermiculite sample[1]	Integrated intensities					r(Al) obs.
	Al^{IV} SSB(2)	Al^{IV} SSB(1)	Al^{IV}	Al*	Al^{VI}	
L_c BAF50	14.8	11.8	44.6 (68)		28.8 (2.5)	0.40
L_cBACl50(b)	2.4	8.8	76.2 (68)		1.5 (9.5) 11.2 (−1.5)	0.15
Intercalated L_cBACl50(b) dried at room temperature	2	7.6	50.9 (67)		2.5 (8.3) 7.5 (−1.7) 18.9 (1)	total 0.48 lattice 0.17
Intercalated L_cBACl50(b) calcined at 500°C			22.7 (68)	29 (31)	38.3 (2)	

[1] See text for descriptions.

The intensity of the spinning side bands (SSB) are taken into account: SBB(i) indicates the ±i° harmonic SSB of the ^{27}Al contribution. Between parentheses is the shift (ppm) of the main lines.

be qualitatively explained in the following way. According to Table 2, the relative CEC of this sample was about 0.6. Thus, the framework relative CEC, or 0.6/(^3Q/Si(t)), was 0.78 for the dealuminated residual framework. If the CEC was entirely saturated by Al^{3+}, (0.78 × 0.9)/3 = 0.23 Al must have been present as $(Al^{3+})^{VI}$ per ½ uc. The net layer negative charge per ½ uc of the original material was 0.9. In the dealuminated structure of the Llano$_c$BACl50(b) sample, 1.16 Al^{IV} and 0.18 Al^{VI} are present per ½ uc, as easily verified by using the data for this sample in Table 2 and Eqs. (5)–(9). Thus, the total Al^{VI} content should have been (0.23 + 0.18) = 0.41, and the ratio Al^{VI}/Al^{IV} should have been 0.41/1.16 = 0.35 instead of the observed of 0.48. The numerical results of the deconvolution procedure are reported in Table 4.

The Al^{VI} resonance of the dry intercalated Llano$_c$BACl50(b) sample clearly contained a sharp peak at about 0 ppm on top of a broad peak. The intensity of the broad contribution divided by the intensity of the framework Al^{IV} contribution yields a Al^{VI}/Al^{IV} ratio of 16%, in close agreement with the r(Al) ratio shown in Table 2. The sharp peak at 0 ppm was most probably the resonance of Al^{3+}.

After thermal activation at 500°C, the ^{27}Al MAS spectrum of the intercalated Llano$_c$BACl50(b) sample changed dramatically. The Al^{IV} resonance contribution broadened to a lesser extent than the Al^{VI} resonance contribution; in addition, another broad contribution appeared at about 30 ppm. If thermal activation had removed the interlayer hydration only, the dehydrated Al^{3+} cations would have been squeezed in the pseudo-hexagonal cavities. Because the Al nucleus was more shielded in this position, its resonance frequencies would have shifted upfield, that is, shifted to <0 ppm, and the resulting line would have broadened, as observed by Laperche *et al.* (1990) for other exchangeable cations, such as Na^{2+} or Cd^{2+} in vermiculite. This may explain the upfield broadening of the Al^{VI} signal in spectrum c. The framework Al^{VI} resonance was centered at about 3 ppm.

The new contribution at ~30 ppm has been observed on thermal activation of layered silicic acid that had intercalated Al moieties (see, e.g., Deng *et al.* (1989) and references therein). This contribution was assigned to pentacoordinated Al. The observation of this peak in the spectra of intercalated vermiculite suggests that a fraction of the intercalated Al was not present as Al^{3+}, but as slabs of polymeric units. Such a suggestion is in line with the formation of ill-defined interstratified structures having relatively high surface areas.

The question now arises as to why the charge-depleted vermiculite did not intercalate the Al_{13} polymer, but instead adsorbed selectively either Al^{3+} or oligomer with higher charge per Al than Al_{13}. In dealuminated vermiculite, the $(Al/Si)^{IV}$ ratio was always greater than ~0.3. The $(NH_4)_2SiF_6$ reagent increased the $(Si/Al)^{IV}$ ratio from 2.2 in the initial sample to about 3.3 in the most dealuminated Llano sample. Though noticeable, this increase is less than that reported in the original patent for zeolites (Breck *et al.*, 1985); e.g., in zeolite Y having an initial $(Si/Al)^{IV}$ ratio of 2.15 (close to that of vermiculite), dealumination treatment "a" yielded a final ratio of 4.15.

In phyllosilicates having Al substitutions in tetrahedral sites, the negative charge on the oxygens in the basal planes was higher than in smectites having octahedral substitutions. In other words, the charge is more localized. The failure of intercalating dealuminated vermiculites with Al_{13} suggests that the localization of negative charge on basal oxygens prevented the intercalation from being selective for the Al_{13} polymer. Beyond some threshold, which must correspond to a $(Si/Al)^{IV}$ ratio <7.7 (the beidellite ratio), the selectivity in the cationic exchange switched in favor of Al^{3+} or oligomeric Al species to achieve a better local neutralization of the localized negative charge. Thus, to insure a better local electroneutrality, the nominal charge per Al must have increased and therefore the equilibrium in reaction (13) shifted to the right.

SUMMARY AND CONCLUSIONS

If, as suggested above, the reaction of $(NH_4)_2SiF_6$ with vermiculite has the side effect of translocating Al

from Al^{IV} to Al^{VI} within the structure by the removal of magnesium, the $(Si/Al)^{IV}$ ratio cannot be increased beyond a limit of about 4. Indeed, to extract Al from the tetrahedral layer, the reagent must have access to the interlayer. In other words, the layered silicate must retain its swelling property.

Consider a hypothetical but realistic vermiculite, of composition $M^{+}_{1.05}[Si_{2.75}Al_{1.25}]^{IV}[Mg_{2.8}Al_{0.2}]^{VI}O_{10}(OH)_2$. Such a structure would be neutral and unable to swell when the following composition is reached $[Si_{3.28}Al_{0.72}]^{IV}[Mg_{2.28}Al_{0.72}]^{VI}O_{10}(OH)_2$, with $(Si/Al)^{IV} = 4$. The consequence of the Al translocation is to prevent the $(Si/Al)^{IV}$ ratio from increasing beyond a limit at which swelling is no longer possible. Thus, dealumination of the tetrahedral layer should stop if the Al^{IV} content, x, exceeds 0.72 or if $(Si/Al)^{IV} \gtrsim 4$.

Assume now that dealumination proceeds to the point where the framework CEC is about 90 meq/100 g, corresponding to the idealized composition

$$M^{+}_{0.45}[Si_{3.05}Al_{0.95}]^{IV}[Mg_{2.5}Al_{0.5}]^{VI}O_{10}(OH)_2 \text{ with } (Si/Al)^{IV} = 3.2,$$

compared with the idealized composition of dioctahedral beidellite,

$$M^{+}_{0.45}[Si_{3.55}Al_{0.45}]^{IV}[Al_2]^{VI}O_{10}(OH)_2.$$

Per oxygen in the basal plane, the excess negative charge is either 0.16 for dealuminated vermiculite or 0.07 for beidellite. In vermiculite, 0.08 positive charge exists per O or OH in the octahedral layer. The internal compensation of the negative and positive charge in vermiculite leads to the same framework charge as in beidellite. In both minerals, the interlayer exchangeable cations attracts the negative charge of the basal plane. In vermiculite they also repulse the positive charge on the O and OH of the octahedral mid-layer plane. Thus, locally, the interlayer cations are in contact with basal planes bearing a density of negative charge twice as large in dealuminated vermiculite as in beidellite. This higher local negative charge calls for a higher density of positive charge in the interlayer cation. With monovalent cations, this requirement is met. With bulky cations, such as Al_{13}, which has a cross-sectional area of ~110 Å^2 and an overall charge between 4+ and 7+ (Bottero *et al.*, 1982), the nominal charge per Al in the intercalated species is not large enough, and either Al^{3+} or oligomers having higher charge per Al than Al_{13} are intercalated.

The intercalation of smaller Al moieties prevents the formation of galleries regularly propped apart by ~8 Å. Instead, smaller and randomly distributed spacings are obtained.

ACKNOWLEDGMENTS

We acknowledge the financial support of Elf Technologies, Inc., Washington, D.C., which made this study possible. An NSF grant (DIR-87 19 808) and an NIH grant (RR 04095), which partly supported the purchase of the GN-500 NMR instrument, are gratefully acknowledged. We want also to thank Fred Mumpton for the considerable amount of time he spent editing our manuscript.

REFERENCES

Angino, E. E. and Billings, G. K. (1972) *Atomic Absorption Spectrometry in Geology*: Elsevier, Amsterdam, 96–97.

Bain, D. C. and Smith, B. F. L. (1987) Chemical analysis: in *A Handbook of Determinative Methods in Clay Mineralogy,* M. J. Wilson, ed., Chapman and Hall, New York, 258–260.

Bottero, J.-Y., Marchal, J. P., Poirier, J.-E., Cases, J., and Fiessinger, F. (1982) Etude par RMN de l'^{27}Al des solutions diluées de chlorure d'aluminium partiellement neutralisées: *Bull. Soc. Chim. Fr.* **11-12,** 439–444.

Breck, D. W., Blass, H., and Skeels, G. W. (1985) Silicon substituted zeolite compositions and process for preparing same: *U.S. Patent* **4,503,023,** 27 pp.

de la Calle, C. and Suquet, H. (1988) Vermiculite: in *Hydrous Phyllosilicates, Reviews in Mineralogy* **19,** W. Bailey, ed., Mineralogical Society of America, Washington, D.C., 455–496.

Deng, Z., Lambert, J.-F., and Fripiat, J. J. (1989) Pillaring puckered layer silicates: *Chemistry of Materials* **1,** 640–650.

Farrah, G. H. and Moss, M. L. (1966) Aluminum: in *Treatise on Analytical Chemistry, Part II, Section A, Volume 4.,* I. M. Kolthoff, P. J. Elving, and E. B. Sandell, eds., Wiley, New York, 405–406.

Herrero, C. P. (1985) Monte Carlo simulation and calculation of electrostatic energies in the analysis of Si-Al distribution in micas: in *Proc. Int. Clay Conf., Denver, 1985,* L. G. Schultz, H. van Olphen, and F. A. Mumpton, eds., The Clay Minerals Society, Bloomington, Indiana, 24–30.

Laperche, V., Lambert, J.-F., Prost, R., and Fripiat, J. J. (1990) High resolution solid-state NMR of exchangeable cations in the interlayer surface of a swelling mica: ^{23}Na, ^{111}Cs and ^{133}Cd vermiculites: *J. Phys. Chem.* **94,** 8821–8831.

Linke, W. F. (1965) *Solubilities: Inorganic and Metal-Organic Compounds, Vol. 2*: American Chemical Society, Washington, D.C., 1914 pp.

López Gonzalez, J. D. and Barrales Rienda, J. M. (1972) Caracterizacion y propiedades de una vermiculita de Benahavis (Malaga): *Anales de Quimica* **68,** 247–262.

Man, P. P., Peltre, M. J., and Barthomeuf, D. (1990) Nuclear magnetic resonance of the dealumination of an amorphous silica-alumina catalyst: *J. Chem. Soc. Faraday Trans.* **86,** 1599–1602.

Miyake, M., Komarneni, S., and Roy, R. (1987) Dealumination of zeolites and clay minerals with $SiCl_4$ or $(NH_4)_2SiF_6$: *Clay Miner.* **22,** 367–371.

Plee, D. (1984) Synthèse et caractérisation des composés d'insertion de smectites: Ph.D. Thesis, Université d'Orléans, Orléans, France, 109 pp.

Plee, D., Borg F., Gatineau, L., and Fripiat, J. J. (1985) High-resolution solid-state ^{27}Al and ^{29}Si nuclear magnetic resonance study of pillared clays: *J. Amer. Chem. Soc.* **107,** 2363–2369.

Plee, D., Gatineau, L., and Fripiat, J. J. (1987) Pillaring processes of smectites with and without tetrahedral substitution: *Clays & Clay Minerals* **35,** 81–88.

Rausell-Colom, J. A., Fernandez, M., Serratosa, J. M., Alcover, J. F., and Gatineau, L. (1980) Organisation de

l'espace interlamellaire dans les vermiculites monocouches et anhydres: *Clay Miner.* **15,** 37–57.

Schutz A., Stone, E. E., Poncelet, G., and Fripiat, J. J. (1987) Preparation and characterization of bidimensional zeolitic structures obtained from synthetic beidellite and hydroxy-aluminum solutions: *Clays & Clay Minerals* **35,** 251–261.

Thompson, K. C. and Reynolds, R. J. (1978) *Atomic Absorption Spectroscopy: A Practical Guide*: Wiley, New York, 319 pp.

(Received 5 June 1990; accepted 2 April 1991; Ms. 2017)